Anal. Chem. **2008,** *80,* 6023–6028

Resolution of Cross-Type Optical Particle Separation

Sang Bok Kim, Sang Youl Yoon, Hyung Jin Sung,* and Sang Soo Kim*

Department of Mechanical Engineering Korea Advanced Institute of Science and Technology 373-1, Guseong-dong, Yuseong-gu, Daejeon, 305-701, Korea

A real-time, continuous optical particle separation method, termed cross-type optical particle separation, is investigated theoretically and experimentally. The trajectory of a particle subject to cross-type optical particle separation is predicted by solving the particle dynamic equation and compared with experimental data. For various flow velocities and particle sizes, the retention distances are measured where the displacement perpendicular to the fluid flow direction is referred to as the retention distance. The measured retention distances are in good agreement with theoretical predictions. The retention distance increases as the particle size increases due to the radiation force, but decreases as the flow velocity increases since the residence time of a particle in the laser beam decreases with increasing flow velocity. To evaluate the performance of the cross-type optical particle separation method, size-based separation resolution is derived theoretically in terms of the refractive index of the particle and instrumental fluctuations. Furthermore, an expression for the maximum resolution is derived.

As light passes through an object, the photon momentum changes, and this change in momentum exerts radiation forces on the object due to Newton's third law.[1] Since the 1970s, this change in photon momentum and the associated radiation forces have been studied experimentally and theoretically.[1–8] Because radiation forces act on an object without physical contact, they have proven to be invaluable tools for manipulating and separating particles and biological cells. The radiation forces consist of a scattering force pointing in the direction of the light and a gradient force acting in the direction of the light intensity gradient.[1] The application of radiation forces can be categorized as manipulation or separation depending on whether the gradient or scattering force is used, respectively.

Nowadays, the manipulation of biological cells using radiation forces, implemented using devices known as optical tweezers, is now well established in biological research.[2,3] Recently, much attention has been devoted to separate particles using radiation forces.[9–12] In particular, particle separation is one of the essential requirements for micro total analysis systems.[13,14] Several techniques, including capillary electrophoretic,[15] dielectrophoretic,[16] and hydrophoretic separation,[17] have recently been developed to separate particles or cells in microscale devices.

Compared to other separation methods, separation using radiation forces has some advantages. A geometrically simple channel can be used, pretreatment of the medium containing the particles is not required, and fluorescent or scattering signals of particles can be detected simultaneously. Imasaka et al. developed optical chromatography, a particle separation method based on a very simple feature.[9] In optical chromatography, the scattering force acts in the direction of laser beam propagation, and the fluid drag force acts on particles in the opposite direction. When the scattering and drag forces are equal, the particles remain stationary. However, separation in optical chromatography is not continuous because the separated particles stay at their equilibrium positions. Optical chromatography has been successfully used to separate biological cells[11] and to enhance the concentrations of colloidal and biological samples in a microdevice.[12] Kim et al. developed a cross-type optical particle separation method that can separate particles continuously.[18] In this method, the particle flow is illuminated with a laser light beam of predetermined width, with the beam oriented perpendicular to the flow direction. As a particle moves through the zone illuminated by the laser, its trajectory is deflected due to the scattering force, such that when the particle exits the illumination zone it is moving in the same direction but its trajectory has been shifted by a distance referred to here as the retention distance. However, although Kim et al. demonstrated

* To whom correspondence should be addressed. E-mail: hjsung@kaist.ac.kr e-mail; sskim@kaist.ac.kr.

(1) Ashkin, A. *Biophys. J.* **1992**, *12*, 569–582.
(2) Ashkin, A.; Dziedzic, J. M. *Science* **1987**, *235*, 1517–1520.
(3) Wang, M. M.; Tu, E.; Raymond, D.; Yang, J. M.; Zhang, H.; Hagen, N.; Dees, B.; Mercer, E. M.; Forster, A. H.; Kariv, I.; Marchand, P. J.; Butler, W. F. *Nat. Biotechnol.* **2005**, *23*, 83–87.
(4) Kim, J. S.; Lee, S. S. *J. Opt. Soc. Am.* **1983**, *73*, 303–312.
(5) Barton, J. P.; Alexander, D. R.; Schaub, S. A. *J. Appl. Phys.* **1989**, *66*, 4594–4602.
(6) Gauthier, R. C. *Appl. Phys. Lett.* **1996**, *69*, 2015–2017.
(7) Gauthier, R. C. *Appl. Opt.* **1998**, *37*, 6421–6431.
(8) Kim, S. B.; Kim, S. S. *J. Opt. Soc. Am. B* **2006**, *23*, 897–903.
(9) Imasaka, Y.; Kawabata, Y.; Kaneta, T.; Ishidzu, Y. *Anal. Chem.* **1995**, *67*, 1763–1765.
(10) Kaneta, T.; Ishidzu, Y.; Mishima, N.; Imasaka, T. *Anal. Chem.* **1997**, *69*, 2701–2710.
(11) Hart, S. J.; Terray, A.; Leski, T. A.; Arnold, J.; Stroud, R. *Anal. Chem.* **2006**, *78*, 3221–3225.
(12) Hart, S. J.; Terray, A.; Arnold, J.; Leski, T. A. *Opt. Express* **2007**, *15*, 2724–2731.
(13) Reyes, D. R.; Iossifidis, D.; Auroux, P. A.; Manz, A. *Anal. Chem.* **2002**, *74*, 2623–2636.
(14) Reyes, D. R.; Iossifidis, D.; Auroux, P. A.; Manz, A. *Anal. Chem.* **2002**, *74*, 2637–2652.
(15) Rodriguez, M. A.; Armstrong, D. W. *J. Chromagtogr., B* **2004**, *800*, 7–25.
(16) Das, C. M.; Becker, F.; Vernon, S.; Noshari, J.; Joyce, C.; Gascoyne, P. R. C. *Anal. Chem.* **2005**, *77*, 2708–2719.
(17) Choi, S.; Park, J. K. *Lab Chip* **2007**, *7*, 890–897.
(18) Kim, S. B.; Kim, J. H.; Kim, S. S. *Appl. Opt.* **2006**, *45*, 6919–6924.

10.1021/ac800740b CCC: $40.75
Published on Web 07/04/2008

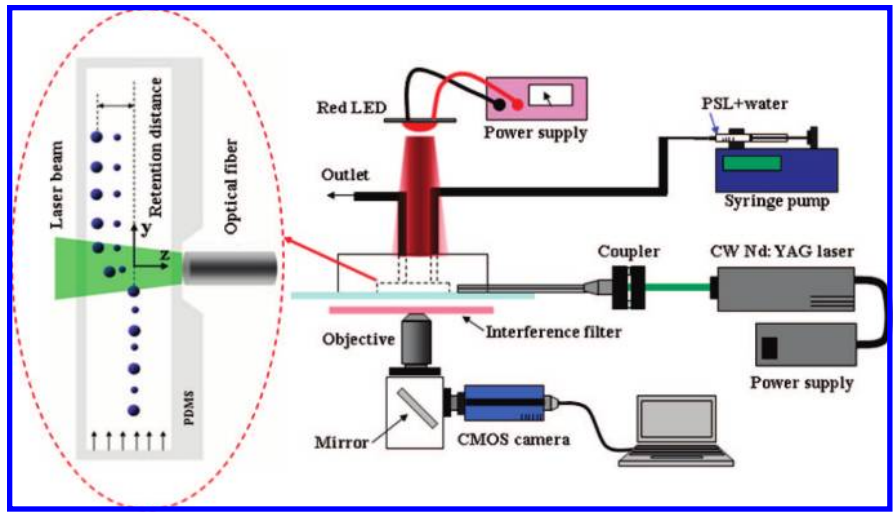

Figure 1. Schematic of the cross-type optical particle separation.

the feasibility of the cross-type optical particle separation method, they only tested one flow condition.[19]

In the present study, the trajectory of a particle moving into and out of a laser beam, as in the cross-type optical particle separation method, was predicted and calculated by solving the particle dynamic equations derived from the ray-optics model. The calculated particle trajectories were compared with experimental data. The spatially averaged retention distances of three different-sized particles were measured under various flow conditions. Furthermore, the size-based resolution of the cross-type optical particle separation method was derived theoretically and the performance of the method was evaluated.

THEORY

To derive the radiation force equation for particles larger than the wavelength of illuminating laser light, a ray-optics model is adopted to calculate the trajectory of a particle and to evaluate the resolution of cross-type optical particle separation. According to Kim and Kim, the scattering and gradient forces on a transparent sphere can be expressed as,[8]

$$F_s = \frac{n_0 d_p^2}{8c}\int_0^{2\pi}\int_0^{\pi/2} I(\rho,z)\,Q_s(\theta)\,\sin 2\theta\,\mathrm{d}\theta\mathrm{d}\phi \qquad (1)$$

$$F_g = \frac{n_0 d_p^2}{8c}\int_0^{2\pi}\int_0^{2\pi} I(\rho,z)\,Q_g(\theta)\,\sin 2\theta\,\cos\phi\,\mathrm{d}\theta\,\mathrm{d}\phi \qquad (2)$$

where F_s and F_g are the scattering and gradient forces, n_0 is the refractive index of the medium, d_p is the particle diameter, $I(\rho, z)$ is the intensity distribution of laser light, ρ is the distance between the center of the sphere and the laser beam axis, z is the axial distance from the waist of the laser beam, Q_s and Q_g are dimensionless efficiencies of the momentum change of photons in the scattering and gradient force directions, respectively, θ is the incident angle of the ray with respect to the normal direction of the sphere's surface, and is φ the polar angle.

In cross-type optical particle separation, particles are irradiated by laser light that is propagating in the direction perpendicular to the fluid flow, as shown in Figure 1. Because micrometer-sized particles are examined in the present study, Brownian motion of particles can be neglected. The dynamic equation for a particle subjected to cross-type optical particle separation can be written as,

$$m_p\frac{\mathrm{d}^2\mathbf{V}}{\mathrm{d}t^2} - 3\pi\mu d_p(\mathbf{U}-\mathbf{V}) = \mathbf{F} \qquad (3)$$

$$\frac{\mathrm{d}\mathbf{r}}{\mathrm{d}t} = \mathbf{V} \qquad (4)$$

where $m_p$is the particle mass, $\mathbf{F}$ is the radiation force vector, $\mathbf{r}$ is the particle position vector, μ is the dynamic viscosity of the fluid, and $\mathbf{V}$ and $\mathbf{U}$ are the particle and fluid velocity vectors, respectively. In Figure 1, the velocities and radiation forces are defined as

$$\mathbf{V} = V_y\hat{\mathbf{y}} + V_z\hat{\mathbf{z}},\ \mathbf{U} = U\hat{\mathbf{z}},\ \mathbf{F} = F_g\hat{\mathbf{y}} - F_s\hat{\mathbf{z}},\ \mathbf{r} = y\hat{\mathbf{y}} + z\hat{\mathbf{z}} \qquad (5)$$

where $\hat{y}$ and $\hat{z}$ are the unit vectors in the y and z directions, respectively. Using the following dimensionless variables

$$\mathbf{V}^* = \frac{\mathbf{V}}{\omega_0/\tau},\ \mathbf{U}^* = \frac{\mathbf{U}}{\omega_0/\tau},\ \mathbf{F}^* = \frac{\mathbf{F}}{m_p\omega_0/\tau^2},\ \mathbf{r}^* = \frac{\mathbf{r}}{\omega_0},\ t^* = \frac{t}{\tau},\ d\mathrm{p}^* = \frac{d_p}{\omega_0} \qquad (6)$$

the dimensionless governing equations can be rewritten as

$$\frac{\mathrm{d}\mathbf{V}^*}{\mathrm{d}t^*} - (\mathbf{U}^*-\mathbf{V}^*) = \mathbf{F}^*,\ \frac{\mathrm{d}\mathbf{r}^*}{\mathrm{d}t^*} = \mathbf{V}^* \qquad (7)$$

where ω_0 is the waist radius of the laser beam and τ is the particle relaxation time, which is denoted as $m_p/(3\pi\mu d_p)$. To solve the above equations, the numerical scheme developed for integration of the Langevin equation was used.[20] Assuming that the radiation forces are constant during a time step, eq 7 can be solved analytically,[20]

$$\mathbf{V}^* = \mathbf{V}_0^* e^{-t^*} + (\mathbf{F}_0^* + \mathbf{U}^*)(1 - e^{-t^*}) \qquad (8)$$

(19) Kim, S. B.; Yoon, S. Y.; Sung, H. J.; Kim, S. S. *Anal. Chem.* **2008**, *80*, 2628–2630.

(20) Ermak, D. L.; Buckholz, H. *J. Comput. Phys.* **1980**, *35*, 169–182.

$$\mathbf{r}^* = \mathbf{r}_0^* + [\mathbf{V}^* + \mathbf{V}_0^* - 2(\mathbf{F}_0^* + \mathbf{U}^*)]\left(\frac{1 - e^{-t^*}}{1 + e^{-t^*}}\right) + (\mathbf{F}_0^* + \mathbf{U}^*)t^* \quad (9)$$

where $\mathbf{F}_0^*$ is a nondimensional constant radiation force vector and $\mathbf{V}_0^*$ and $\mathbf{r}_0^*$ are the initial values of the nondimensional particle velocity and position vectors, respectively. From eqs 8 and 9, the discretized governing equations of particle motion can be derived as

$$\mathbf{V}_{n+1}^* = \mathbf{V}_n^* e^{-\Delta t^*} + (\mathbf{F}_n^* + \mathbf{U}^*)(1 - e^{-\Delta t^*}) \quad (10)$$

$$\mathbf{r}_{n+1}^* = \mathbf{r}_n^* + \left[\mathbf{V}_{n+1}^* + \mathbf{V}_n^* - 2(\mathbf{F}_n^* + \mathbf{U}^*)\right]\left(\frac{1 - e^{-\Delta t^*}}{1 + e^{-\Delta t^*}}\right) + (\mathbf{F}_n^* + \mathbf{U}^*)\Delta t^* \quad (11)$$

where n denotes the time level and Δt^* is the nondimensional time step.

EXPERIMENTAL SETUP

A schematic of the experimental setup is shown in Figure 1. The polydimethylsiloxane (PDMS) microchannel, which was fabricated using conventional photolithography, had a channel width and height of 210 and 100 μm, respectively. Through an optical fiber (MMF-31-IRVIS-50/125, NA = 0.22 Oz Optics), a Nd:YAG continuous wave laser operating at wavelength 532 nm was delivered into the microchannel and exerted the radiation force on particles in a direction perpendicular to the direction of the fluid flow. Initially, particles move parallel to the direction of fluid flow. As the particles pass through the region irradiated by the laser beam, however, their trajectories are deflected due to the scattering force, which pushes the particles in the direction of laser beam propagation. When the particles exit the laser beam region, their positions have been changed in the direction of laser beam propagation with respect to their initial positions in the flow. This position change of the particles, which is termed the retention distance, is greater for larger particles.

Using a CMOS camera (pco.1200hs), an objective lens (20×), and a mirror, an inverted microscope was set up as shown in Figure 1. The microchannel and optical fiber system were mounted on a microstage and combined with the inverted microscope. To obtain clear images of the particle trajectories, scattered light from the laser was removed using an optical interference filter (F10-632.8-4-2.00, CVI Optics), and a red LED was adopted as a light source for image capture. Finally, the flow system was constructed using a 1-mL gastight syringe (81320, Hamilton), a syringe pump (pump 11, Harvard apparatus), and a poly(tetrafluoroethylene) tube. The flow velocity was controlled by the syringe pump from 100 to 700 μm/s. Three distinct sizes of polystyrene latex (PSL) (Duke Scientific Corp.) particles were used: 2.0 μm ± 0.02 μm, 5.0 μm ± 0.05 μm, and 10.0 μm ± 0.09 μm (in diameter). All PSL particles had a refractive index of 1.59. The particles were suspended in water and introduced into the microchannel. During the experiments, the waist radius and power of the laser beam were kept constant at 40 μm and 1 W, respectively.

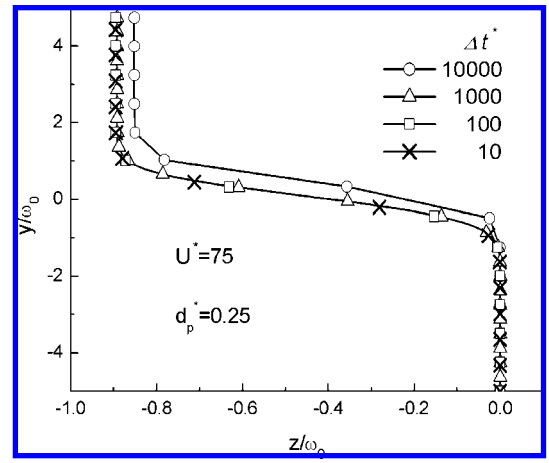

Figure 2. Numerical simulation of trajectory of particle $d_p^* = 0.25$ with flow velocity $U^* = 75$. The simulated trajectories are converged when Δt^* is less than 1000.

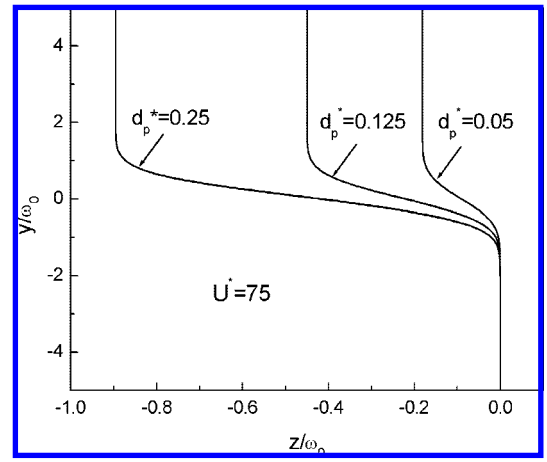

Figure 3. Numerical simulation of trajectories of three distinct sized PSL particles.

RESULTS AND DISCUSSION

Particle Trajectory. Trajectories of particles subject to cross-type optical particle separation are simulated using the actual experimental conditions, such as laser beam width and power, flow velocity, and particle sizes. To determine an appropriate nondimensional time step, a convergence test was performed. Because the radiation force increases as the particle size increases, the largest particle size used in the experiments ($d_p^* = 0.25$) was considered in the convergence test. As shown in Figure 2, the trajectory converges when the nondimensional time step is less than 1000. Assuming a true solution is obtained when the nondimensional time step is $\Delta t^* = 10$, the relative errors at $\Delta t^* = 1000$ and 100 are less than 0.4 and 0.04%, respectively. Thus, the nondimensional time step $\Delta t^* = 100$ is employed for all simulations.

Trajectories of particles with three sizes, $d_p^* = 0.05$, 0.125, and 0.25, are shown in Figure 3. Initially, the particles suspended in the fluid move parallel to the direction of fluid flow. As the particles pass through the laser beam, however, the scattering force pushes them in the direction of laser beam propagation, which is perpendicular to the fluid flow direction. After the particles exit the laser beam irradiation region, they again move parallel to the fluid flow direction. During these deflected trajectories, the z-directional displacement z_r (i.e., the retention distance) is

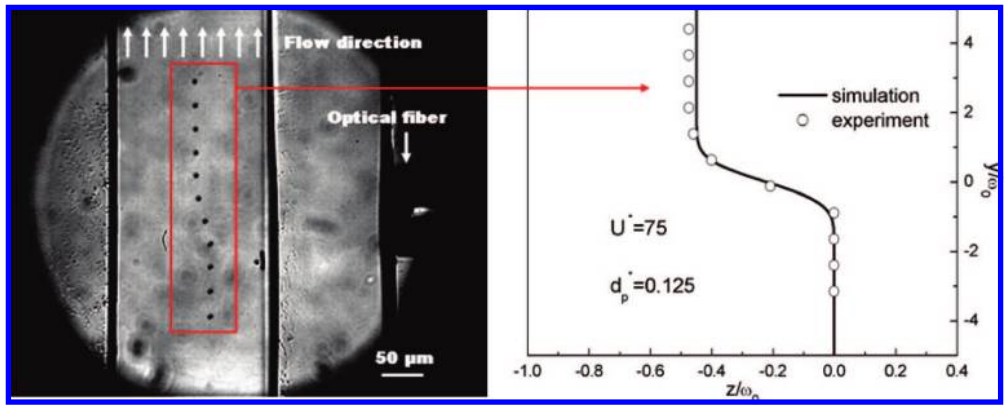

Figure 4. Comparison between experimentally measured and theoretically predicted particle trajectory. Numerical simulation and experimental conditions.

apparent. Since the radiation force depends on the particle size, the retention distance also depends on the particle size. The detailed dependence of the retention distance on the particle size is discussed in the following section. Simulated and experimentally measured particle trajectories are compared in Figure 4 for the particle size of 5 μm ($d_p^* = 0.125$) and the flow velocity of 300 μm/s ($U^* = 75$). As shown in Figure 4, the simulation results are in good agreement with the experimental data.

Retention Distance. To predict the retention distance for various particle sizes and experimental conditions, Kim et al. derived an analytical expression for the retention distance by assuming a spatially averaged scattering force using a ray-optics model.[18] Under their spatially averaged scattering force approximation, the intensity distribution of the laser beam is assumed to be Gaussian. The retention distance derived on the basis of the spatially averaged scattering force is written as[18]

$$z_r^* = \frac{z_r}{\omega_0} = \left(\frac{n_o P}{6\pi\mu U c \omega_0}\right) d_p^* Q^* \sqrt{\frac{\pi}{2}}\,\mathrm{erf}(\sqrt{2}) = S^* d_p^* Q^* \sqrt{\frac{\pi}{2}}\,\mathrm{erf}(\sqrt{2}) \tag{12}$$

where n is the refractive index of the medium, P is the power of the laser beam, c is the speed of light in a vacuum, Q^* is a constant that depends on the refractive indices of the particle and medium, erf denotes the error function, and S^* is a nondimensional parameter that represents the term in parentheses. Equation 12 can be derived using eqs 8 and 9 by using the spatially averaged scattering force, which does not depend on the particle position, instead of the radiation force term, which depends on the particle position.

To validate eq 12, eqs 8 and 9 are solved with and without the gradient force. Figure 5 shows particle trajectories calculated with and without the gradient force for a system with $d_p^* = 0.125$ and $U^* = 75$. As shown in Figure 5, the effect of the gradient force is negligible. Since the laser beam width is much greater than the particle size under the present experimental conditions, the particle does not experience the intensity gradient of the laser beam. The effect of the intensity gradient is well established in the literature.[8,10] Therefore, provided the laser beam width is much larger than the particle size, the retention distances can be predicted using eq 12.

Figure 6 shows the measured retention distances and theoretical predictions for various flow conditions and particle sizes. The

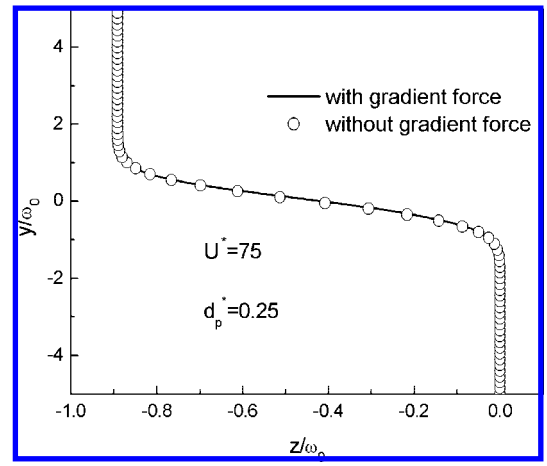

Figure 5. Numerical simulation of trajectory of particle with and without gradient force.

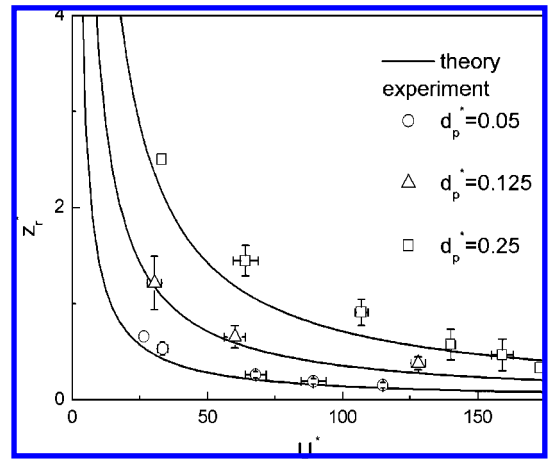

Figure 6. Comparison between experimentally measured and theoretically predicted retention distances.

laser beam width and power were kept constant, as described above. The measured retention distances are in good agreement with the theoretical predictions. Because the residence time of the particles in the laser beam decreases as the flow velocity increases, the retention distance decreases as the flow velocity increases. For a given flow velocity, the retention distance increases with increasing particle size. In the present setup, it takes 0.8−0.1 s for the complete separation of a single particle.

The throughput of the present cross-type optical particle separation is in the range of 1−10 particles/s when a particle passes through the laser beam in a single file. This throughput is lower than that of the current state-of-the-art sorting techniques.[21] However, this value can be increased when a stream of concentrated particles is passing through the laser light.[18,22]

Resolution. The resolution of cross-type optical particle separation is derived analytically. To obtain the proper expression for the resolution, the definition of resolution used in conventional chromatography is employed,[23]

$$\mathrm{Rs} = \frac{2\Delta z}{W_\mathrm{A} + W_\mathrm{B}} = \frac{1}{2}\frac{\Delta z}{\sigma_\mathrm{A} + \sigma_\mathrm{B}} \tag{13}$$

where Δz is the distance between the peaks of the distributions of particles A and B as they are eluted, and W_A and W_B are the widths of the peaks for particles A and B. The respective peak width is equivalent to 4σ, where σ is the standard deviation of the elution time distribution.[23] In cross-type optical particle separation, Δz corresponds to the difference in retention distance between two particles. The standard deviation can be generated by thermal fluctuations and instrumental fluctuations,[10]

$$\sigma_\mathrm{tot}^2 = \sigma_\mathrm{thermal}^2 + \sigma_\mathrm{inst}^2 \tag{14}$$

where σ_thermal and σ_inst are the standard deviations due to thermal and instrumental fluctuations, respectively. The thermal fluctuations can be described as follows in terms of a mass and spring system,[10]

$$\sigma_\mathrm{thermal} = \sqrt{kT/\kappa} \tag{15}$$

where k is Boltzmann's constant, T is the temperature, and κ is a spring constant.[10] Using eq 12, the instrumental fluctuations can be obtained as

$$\sigma_\mathrm{inst} = \frac{\partial z}{\partial P}\Delta P + \frac{\partial z}{\partial U}\Delta U = z_\mathrm{r}\left(\frac{\Delta P}{P} - \frac{\Delta U}{U}\right) = z_\mathrm{r}\left[\frac{\Delta(P/U)}{(P/U)}\right]^{-1} \tag{16}$$

The theory adopted in the present study is based on a ray-optics model, which is suitable for particles with diameters larger than the wavelength of the laser light. Particles with sizes of 1−100 μm are employed. Since this range encompasses the sizes of most biological cells, the cross-type optical particle separation approach can be used to separate biological cells as well as micrometer-sized particles. For particles larger than 1 μm, thermal fluctuations can be neglected. From eqs 12, 13, and 16, the resolution of cross-type optical particle separation can be written as,

$$\mathrm{Rs} = \frac{1}{2}\frac{|d_\mathrm{pA}Q_\mathrm{A}^* - d_\mathrm{pB}Q_\mathrm{B}^*|}{d_\mathrm{pA} + d_\mathrm{pB}}\left[\frac{\Delta(P/U)}{(P/U)}\right]^{-1} \tag{17}$$

The resolution is, therefore, determined by the particle size and refractive index and by instrumental fluctuations.

For particles with the same refractive index, i.e., $Q_\mathrm{A}^* = Q_\mathrm{B}^*$, and a size difference of $d_\mathrm{pA} = d_\mathrm{p} + \Delta d_\mathrm{p}$ and $d_\mathrm{pB} = d_\mathrm{p}$, the size-based separation resolution can be rewritten as,

$$\mathrm{Rs} = \frac{Q^*}{2}\frac{\Delta d_\mathrm{p}/d_\mathrm{p}}{2 + \Delta d_\mathrm{p}/d_\mathrm{p}}\left[\frac{\Delta(P/U)}{(P/U)}\right]^{-1} \tag{18}$$

The size-based separation resolution can be determined by the size difference and instrumental fluctuations. Since the radiation force does not depend on the particle size when the particle diameter is much greater than the laser beam width,[10] the resolution must have a limiting value as the difference in particle size goes to infinity. From eq 18, this limiting value of the resolution can be obtained,

$$\lim_{\Delta d_\mathrm{p}/d_\mathrm{p}\to\infty} \mathrm{Rs} = \frac{Q^*}{2}\left[\frac{\Delta(P/U)}{(P/U)}\right]^{-1} \tag{19}$$

The maximum size-based separation resolution depends on instrumental fluctuations and the refractive index of the particles. For instrumental fluctuations of 0.1% and PSL microspheres, the maximum size separation resolution and eq 19 are plotted in Figure 7. In conventional chromatographic analysis, the commonly used criterion for complete separation is that the resolution greater than 1.5.[23] Figure 8 shows the size separation resolution of PSL particles for systems with various instrumental fluctuations and the criterion of complete separation. For instrumental fluctuations of 0.1%, particles that differ in size by 4% can be resolved. For instrumental fluctuations of 10%, however, complete separation can never be satisfied. The resolution of the present cross-type optical particle separation is lower than that of optical chromatography due to the longer retention distance of optical chromatography.[10] However, the separation time is shorter than that of optical chromatography because particles are decelerated in optical chromatography while the particle velocity is constant in cross-type optical particle separation.

In eq 19, the effect of the refractive index on the resolution is implicitly included in Q^*.[10,18] Since the radiation force increases

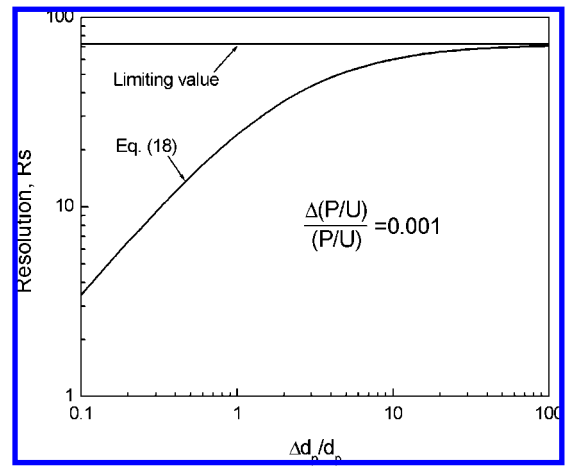

Figure 7. Size-based separating resolution as a function of particle size differences.

(21) Huh, D.; Gu, W.; Kamotani, Y.; Grotberg, J. B.; Takayama, S. *Physiol. Meas.* **2005**, *26*, R73−R98.
(22) Lee, G. B.; Hung, C. I.; Ke, B. J.; Huang, G. R.; Hwei, B. H.; Lai, H. F. *Trans. ASME* **2001**, *123*, 672–679.
(23) Skoog, D. A.; Holler, F. J.; Nieman, T. A. *Principles of instrumental analysis*, 5th ed.; Thomson Learning: London, 1988.

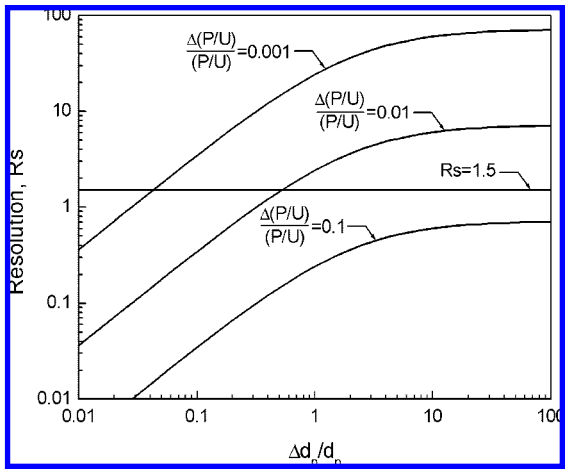

Figure 8. Size-based separating resolution of the cross-type optical particle separation as a function of particle size difference.

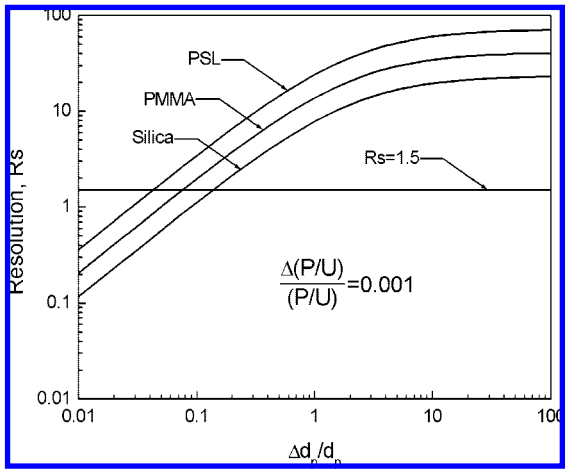

Figure 9. Size-based separating resolution of the cross-type optical particle separation as a function of particle size difference.

as the refractive index increases, the retention distance also increases with increasing refractive index. Therefore, the resolution depends on the refractive index. Figure 9 shows the size-based separation resolution for particles with three distinct refractive indices. In Figure 9, the refractive indices of PSL, poly(methyl methacrylate) (PMMA) and silica particles are 1.59, 1.49, and 1.43, respectively. As expected, a higher resolution can be achieved for particles with a higher refractive index. A histogram is constructed for two different flow velocities ($U^* = 70$ and 120) and two different-sized PSL particles ($d_p^* = 0.05$ and 0.25). As shown in Figure 10, the resolution is almost the same (Rs = 3.0 and 3.1 for $U^* = 70$ and 120, respectively) while measured retention distances are different.

CONCLUSIONS

In the present study, the cross-type optical particle separation method was analyzed theoretically and experimentally. To elucidate the particle behavior, trajectories of different-sized particles were simulated using a ray-optics model. An appropriate integration time step was obtained from a convergence test, and the simulated trajectory was compared with experimental data. The simulation and experimental data were in good agreement.

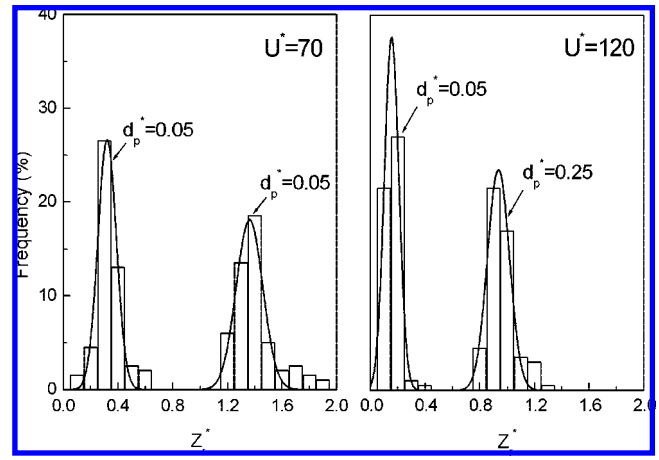

Figure 10. Histogram of retention distance for two different flow conditions.

Retention distances were measured experimentally for systems with various flow velocities and particle sizes. In the experiments, the gradient force was negligible since the width of the laser beam was much larger than the particle size. An analytical expression for the retention distance was derived under the assumption of constant intensity. The retention distance increased linearly with increasing particle size and was proportional to the inverse of the flow velocity. To evaluate the size-based separating performance, a theoretical size-based separation resolution was derived using the definition of resolution employed in conventional chromatography. Neglecting Brownian motion, the size-based separation resolution can be predicted based on the particle properties and instrumental fluctuations. The resolution increases as the size difference between particles increases but converges to a limiting value since the radiation force does not depend on the particle size for particles much larger than the laser beam width. When the particles had different refractive indices but the same size difference, the resolution increased as the refractive index difference increased. The resolution analysis can be used to optimize the design of the particle separation method. Since the cross-type optical particle separation approach has a simple geometry and can separate many particles in a continuous manner, it may be applied to micro total analysis systems for chemical analysis and particle separation. When particle size goes down to the Rayleigh regime, i.e., the particle size is less than the wavelength of the illuminating laser light, the electromagnetic theory should be applied. In the Rayleigh regime, since the scattering force has a sixth power dependence on particle diameter, the sensitivity of the scattering force would be higher than that of the ray-optics regime. However, Brownian motion of particles would decrease the resolution.

ACKNOWLEDGMENT

The authors express their gratitude for support through a grant from the Brain Korea 21 Program of the Ministry of Education.

Received for review April 14, 2008. Accepted June 4, 2008.

AC800740B